Bandwidth Dependency of (O)LEDs on Bias current

*Andrew Burton, [+]Paul Anthony Haigh, [#]Petr Chvojka, *Zabih Ghassemlooy, [#]Stanislav Zvánovec

*Optical Commumications Research Group, Department of Electrical and Electronic Engineering, Faculty of Engineering and Environment, Northumbria University, Newcastle upon Tyne, NE1 8ST, UK

[+]Intelligent sensing and Communications Group, Faculty of Science, Agriculture and Engineering, Newcastle University, Newcastle upon Tyne, NE1 7RU, UK

[#]Wireless and Fibre Optics Group, Department of Electromagnetic Filed, Faculty of Electrical Engineering, Czach Technical University in Prague, Prague 16627, Czech Republic

{andrew2.burton; z.ghassemlooy}@northumbria.ac.uk, Paul.Haigh@newcastle.ac.uk, {petr.chvojka; xzvanove}@fel.cvut.cz

***Abstract*—This work investigates the modulation bandwidth (B_{mod}) dependency of organic and non-organic light emitting diodes (OLED\LED) on the applied bias current (I_B). The equivalent lumped element transient circuit models are shown with the critical components empirically extracted for both types of device. Four OLEDs of varying sizes are tested in addition to four high power LEDs (white phosphor, red, green and blue). Through analysis of the current-voltage characteristics, the device and dynamic diode resistances are determined as well as the ideality factors. We show that OLEDs have higher ideality factors to the traditional LEDs (almost double) hence the increased turn-on voltage, however have similar AC drive voltage characteristics across the emitting portion of the device between 8-12%. Furthermore, both devices exhibit an increase in B_{mod} with an increase in I_B. It is shown that the OLEDs B_{mod} increases linearly in relation to I_B, reaching ≥80% of the maximal B_{mod} at ≥60% of their maximum I_B rating. Conversely, the LEDs display an exponential rise in B_{mod} in relation to I_B, with ≥80% of the maximal B_{mod} at ≥35% of their maximum I_B rating, with the red LED showing the greatest results at just 17%.**

Keywords — visible light communications; OLED; LED; transient analysis; modulation bandwidth.

I. INTRODUCTION

Visible light communications (VLC) is an optical wireless communications subset driven through solid-state lighting; the light emitting diode (LED) [1, 2], LASER diodes [3] and more recently the organic LED (OLED) [4]. Compared to the more traditional radio frequency (RF) communications platform, VLC presents a cost-effective, license-free (~400 THz) bandwidth and immunity to electromagnetic interference. Additionally, the current demand for high-speed wireless connectivity has led to an RF spectrum congestion, hence the migration into the optical domain. This technology also has the capability to combine illumination with data communications, sensing and localization. Therefore, it has the potential to impact not only indoor wireless access and outdoor scenarios such as the intelligent transport system (ITS) [5], but also 5G architectures [6] and the connectivity of all devices in the internet of things (IoT) [7].

As OLED technology continues to mature, these devices are increasingly becoming candidates for use in VLC due to their high brightness, relatively low production costs and comparatively high efficiency [4]. In addition, they have the ability to be manufactured in a multitude of different ways and deposited onto an assortment of bespoke large area substrates, which is in contrast to the point source LED. All this makes the OLED an exciting prospect and hot topic for VLC research. However, due to the low mobility of the organic semiconductors the resultant modulation bandwidth (B_{mod}) has been reported in the range of 10's to 100's of kHz, in contrast to LEDs having B_{mod} in the MHz region. In such bandlimited systems, data capacity enhancements have been achieved using multicolor wavelength division multiplexing (WDM) [8], single wavelength multiple input multiple output (MIMO) [9, 10], spectrally efficient modulation techniques [11] and equalization [12]. Gigabit VLC has been reported using LEDs employing WDM (>15 Gb\s [13]), MIMO (>6 Gb\s [10]) and equalization (2.32 Gb\s [14]).

Similarly, due to their lower modulation bandwidths, OLEDs have achieved lower data rates yet several reasonable rates have been demonstrated [15]. In a VLC consisting of a large area small molecule OLED as a transmitter, a rate of up to 2.7 Mb/s was achieved in spite of the fact that the modulation bandwidth was 93 kHz [16]. Another report showed that the same OLED can achieve a transmission rate of 1 Mb/s when used in combination with an organic photodetector (OPD) [17]. Both of these links required an artificial neural network equalizer in order to achieve such rates. Next, polymer-based LEDs (PLEDs) were used, which have smaller areas and comparatively high bandwidths (in the order of several hundred kHz). These devices were used to achieve a rate of 10 Mb/s for the first time [18] using orthogonal frequency division multiplexing (OFDM). This was subsequently doubled by reverting to the artificial neural network equaliser [19] to 20 Mb/s with an orange wavelength. Extending to wavelength-multiplexing, a rate of ~55 Mb/s could be achieved by using an individual equaliser on each channel [20]. The current record for a high speed link is set at 51.6 Mb/s by [21], using a single wavelength with an optimised OFDM system and an equaliser.

The electrical-to-optical (EO) characteristics of the transmitting devices are essential to understand in order to optimize the VLC systems. This paper experimentally investigates the devices (OLEDs and LEDs) and characterizes them in terms of impedance for efficient driving and maximum power transfer, and the bandwidth dependency on bias current.

978-1-7281-8691-7/20/$31.00

The rest of this paper is organized as follows: the standard (O)LED model and lumped element equivalent model is given in Section II. The experimental setup for the testing of the devices is given in Section III. The results of the DC and AC characterization are given in Sections IV and V respectively. Finally, the conclusions and observations are outlined in Section VI.

II. (O)LED Model

The standard simplified structure and transient model for the (O)LED is shown in Fig. 1(a-b) [22, 23]. Typically, such devices are made from an emissive layer sandwiched between two electrodes, a cathode (-) and an anode (+). For the organic emitter carbon-based small molecules or polymers are used, whereas in general the non-organic emitters are based around Gallium nitride (GaN) compounds. To model the devices, a serial resistance R_S is used at the input representing the contact and neutral region resistances. A parallel shunt resistance R_p, assumed to have a very high value (> MΩ) models the leakage current through the device. The parallel capacitance C_s and C_d (space-charge and diffusion) are non-linear in nature and strongly depend upon the diode current I_D. Likewise, the diode exhibits a non-linear resistive nature with the characteristics of the Shockley diode equation [24], given by:

$$I_D = I_S \exp\left(\frac{q(V_D - I_D R_S)}{nKT} - 1\right), \quad (1)$$

where I_D is the device current, I_S is the reverse bias saturation current, q is the charge of an electron, V_D is the voltage across the device, n is the ideality factor, K is Boltzmann's constant and T is the junction temperature (in Kelvin). Ideality factors contain important informationon the transport and recombination processes in semiconductors [25]. For GaN based diodes it is typically expected to be between 1 and 2, increasing for organic devices [26].

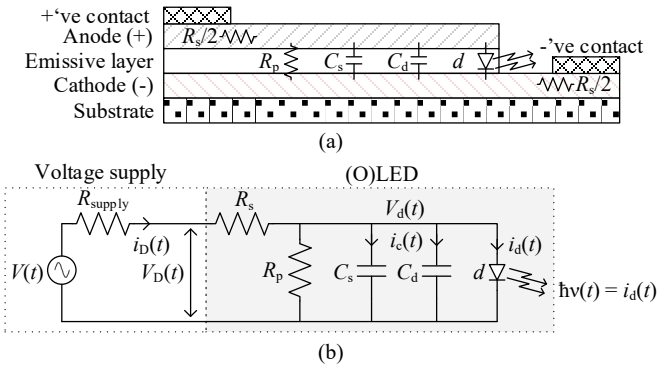

Fig. 1(a) simplified (O)LED structure and (b) model for the electrical to optical transient transfer function.

The 3 dB B_{mod} transient response of the LED is a function of the differential lifetimes, capacitance and I_D expressed by [22]:

$$B_{mod} = \frac{1}{2\pi(\tau_s + \tau_c)}, \quad (2)$$

where τ_s is related to the differential lifetime and inversely proportional to I_D; whereas τ_c is related to the capacitance and is proportional to I_D. Furthermore, when modulating the device with a voltage source, care must be taken to ensure that it is operating in the quasi-linear region of the voltage to optical output power transfer function. This is demonstrated in Fig. 2 (using the G LED), where it shows not only the quasi-linear region but also the turn on and saturation point of the device. Modulating voltage signals above or below these areas will result in non-linear distortion and clipping of the output power.

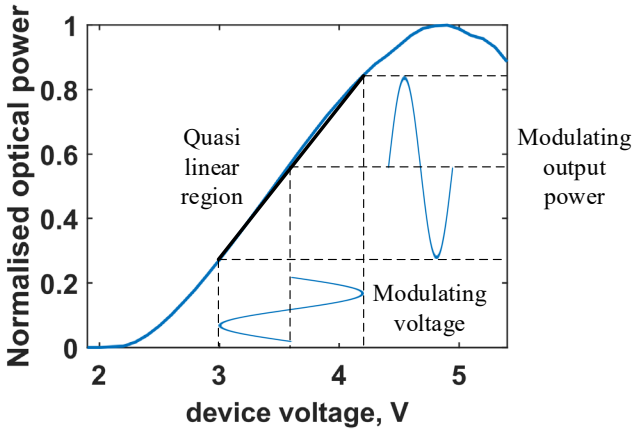

Fig. 2 (O)LED biasing in the quasi linear region and modulating forward voltage to output power transfer.

III. Experimental Setup

The experimental setup to analyse the transient behaviour of the devices under test (DUT) is given in Fig. 3. A laser driver (LD) is used to provide the constant bias current I_B (where $I_B = I_D$) to the devices whereas the arbitrary function generator (AFG) is used to deliver the perturbations $x(t)$. The modulating voltage has been set to a level on each device ensuring that the output signal has not been clipped. Both of the signals are then summed in the bias tee (BT) and used to drive the DUT. Following free-space transmission over a line of sight (LoS) channel, the optical signals are captured and electrically regenerated with the optical receiver (ORx). The regenerated signals $y_{ele}(t)$ are then captured on a digital storage oscilloscope (DSO, Agilent Technologies Infiniium DSO9254A), or spectrally examined on the signal analyzer (SA, Agilent Technologies MXA signal analyzer N92020A). The SA is used to accurately measure the frequency response of each of the DUT, at stepped levels of I_B. The DSO has been employed to capture on-off keying non-return to zero (OOK NRZ) data. This data is taken off-line and the corresponding eye diagrams are plotted in MATLAB.

The DUT are shown in Fig. 4. The OLEDs of varying sizes and power are labelled OLED1 to OLED4 with specifications given from data sheets supplied in Table I. For comparison, off the shelf inorganic gallium based LEDs are also tested. The Luxeon rebel white phosphor (WPLED) and a red, green and blue (RGB) chip LED.

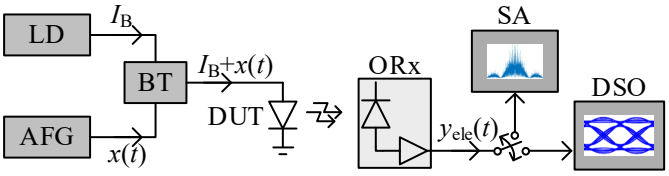

Fig. 3 Experimental block diagram

Fig. 4 The DUT

Table I OLED DUT specifications

DUT	Luminance area (mm)	Typ. luminous efficacy (lm/W) (I_B(mA))
OLED1 (N6OA40-F)	48.7 (Radius)	55 (230)
OLED2 (N6SC40C)	127.2 × 127.2	55 (480)
OLED 3 (N6BA40-B)	191 × 41	53 (230)
OLED4 (N6SB40-B)	46 × 46	55 (62)
WPLED	1.67 (radius)	106 (350)
R, G, B	*Not given*	*Not given*

IV. Device DC Characterisation

Each of the devices has been characterized in terms of the diode equation (Eq. 1). The device current-voltage (I_D-V_D) transfer functions have been accurately measured using a Keithley 2400 SourceMeter®. Fig. 5(a-b) show the I_D-V_D transfer functions for the WPLED and OLED1 devices respectively. The dynamic resistance R_D of the device can be estimated through the inverse tangent of the transfer function at each point along the plot, i.e. $(dI_D/dV_D)^{-1}$. This is shown in the figure as the solid orange line. Likewise, the dynamic resistance of the intrinsic diode r_d for each DUT can be estimated taking the first derivative of the reciprocal of the Shockley diode equation eq(1), i.e. $(dI_d/dV_d)^{-1}$, which yields:

$$r_{\mathrm{d}} = \frac{nv_t}{I_D}, \tag{3}$$

where v_t is the thermal voltage defined by KT/q. The parameter n is found through fitting r_d onto R_D on the left-hand side of the curve (the grey area) where the r_d is the dominant factor of R_D; r_d is shown in the figure as the dashed red line. The plot is shown to be almost constant in the unshaded area. This is due to the exponential current behaviour of the diode. Furthermore, in this region R_S becomes the dominant parameter of R_D. Hence, an estimate of R_S can be made as the difference between R_D and r_d, i.e.:

$$R_S = R_{\mathrm{D}} - r_{\mathrm{d}}. \tag{4}$$

R_S is plotted in the Fig. 5 as the dotted orange line. Thus, at the maximum I_D-V_D measurement an accurate estimate of R_S can be obtained. The estimate for r_d has also been taken at the same point of the curve (as there is little change in this region), and is plotted with R_S in Fig. 5(c). The numerical values are then given in Table II. Additionally, Table II outlines the ratio of R_S to r_d and the percentage of $V_D(t)$ that falls across d (using the voltage divider rule). Examining R_D, it can be seen that the values for the LED DUT ≤ 1 Ω, whereas the OLED DUT exhibit > 2 Ω with the maximum estimate for OLED4 at 8.38 Ω. This implies for both types of device that a driver with similar low R_{spply} is required for maximum power transfer, unlike the standard 50 Ω output of AFG. Moreover, when driven by the AFG, between 8 – 13% of the $V_D(t)$ signal falls across the emitting portion of the DUT with the exception here of the WPLED measured here at almost 24%.

Fig. 5(d) depicts the ideality factor, where it can be seen that the OLEDs have been measured at almost double to that of the LEDs meaning that they require a higher turn-on voltage.

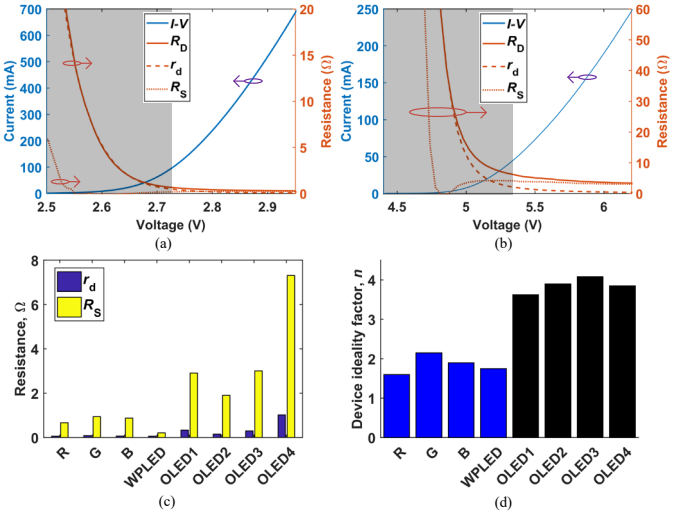

Fig. 5 DUT DC characterization, I-V curves for (a) WPLED, (b) OLED1; (c) the extracted diode characteristic resistance, and (c) diode ideality factor.

Table II DUT estimates of R_D, R_S and r_d

DUT	R_D (Ω)	R_S (Ω)	r_d (Ω)	R_S/ r_d (Ω/ Ω)	$r_d/(R_S+r_d)$*100
R	0.733	0.672	0.061	11.016	8.322
G	1.030	0.945	0.085	11.118	8.252
B	0.952	0.880	0.072	12.200	7.563
WPLED	0.286	0.219	0.067	3.269	23.427
OLED1	3.266	2.917	0.349	8.358	10.686
OLED2	2.069	1.911	0.158	12.095	7.637
OLED3	3.316	3.005	0.311	9.662	9.379
OLED4	8.380	7.305	1.075	6.795	12.823

V. Device AC Characterisation

For the AC characterization of the DUT, the setup shown in Fig. 3 has been used. The output of the ORx was connected to the SA and the AFG was used to sweep frequencies in order to measure the response of the DUT at different levels of I_B. The experiment was repeated for each level of I_B and every device. Figs. 6(a) and (c) show the results for the WPLED and OLED1 respectively. Each of the curves has been normalised to 0 dB at the start of the measurements in order to compare the -3 dB B_{mod} points for each I_B. Figs. 6(b) and (d) plot the relationship between the measured B_{mod} and I_B for the WPLED and OLED1 respectively.

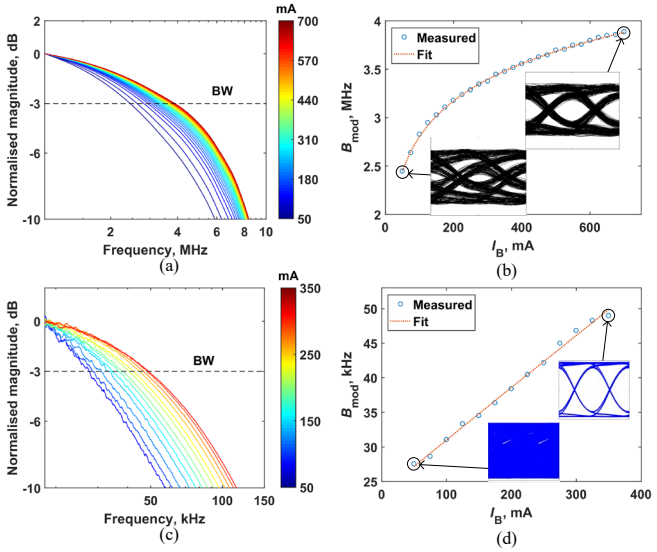

Fig. 6 DUT transient analysis, measured frequency response with stepped I_B for (a) WPLED and (c) OLED1; and extracted B_{mod} vs. I_B for (b) WPLED (inset eyediagrams at 10 Mb/s for min and max I_B) and (d) OLED1 (inset eyediagrams at 100 kb/s for min and max I_B).

The fit curve has been plotted using the MATLAB curve-fitting tool and the two-term power series model ($f(x) = ax^b + c$). Interestingly, the WPLED displays an exponential rise in B_{mod} tending towards a saturation level as I_B increases. On the other hand, OLED1 has been observed to display a linear rise in B_{mod} with respect to I_B without any sign of saturation. Hence, as OLED technology matures and devices are made to operate at higher currents, the B_{mod} should also continue to rise to the higher kHz and into the MHz region. Inset into Figs. 5(b) and (d) are the eye diagrams for pseudo-random bit sequences (PRBS) of length 2^{10}-1 of on-off keying non-return to zero (OOK NRZ) data captured on the DSO and analyzed offline in MATLAB, at data rates of 10 Mb/s and 100 kb/s respectively at the lowest and highest I_B. The eye diagram for the WPLED shows a clear eye-opening at full I_B and only a partial opening at the minimum. Likewise, OLED1 displays a full eye-opening with the maximum current and a completely closed eye with the minimum.

Using the fitted curves for the DUT, a comparison has been made normalizing each of the sets of I_B and the associated B_{mod} to unity, and is shown in Fig.7. The figure shows that each of the OLEDs under test displays the same linear trend transfer function. Likewise, the LEDs also display a similar exponential rise to their transfer functions tending towards a saturation point. These two different behaviours indicate that the LEDs DUT biased to ≥35% of their maximum rating offer ≥80% of the maximal available BW. Conversely, the OLED DUT requires biasing to ≥60% of their maximum rating in order to offer ≥80% of the maximal available BW. However, biasing the OLEDs to a high level in a communication system can introduce nonlinear effects on the signal due to the saturation limit on the optical output power. These effects are more severe on the multilevel and analogue modulation schemes (such as multiple carrierless and phase modulation (*m*-CAP) [27] or orthogonal frequency division multiplexing (OFDM) [28]), than on binary level modulation such as OOK or pulse position modulation (PPM). Furthermore, having to biasing at a high level can be detrimental to the overall lifetime of the device.

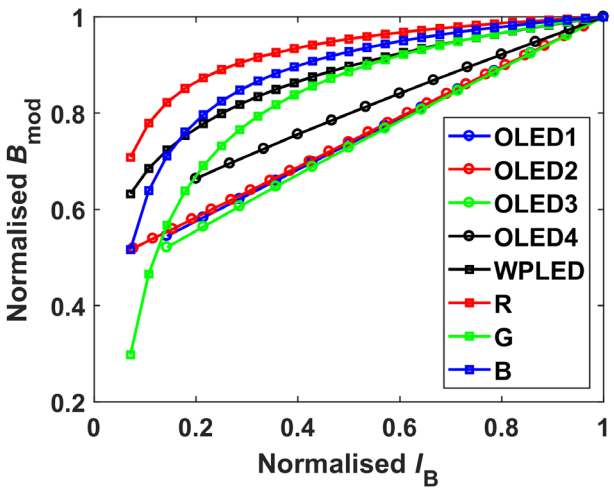

Fig. 7 Comparison of the normalised B_{mod} vs. normalised I_B of the DUT.

VI. Conclusion

This work has investigated a set of four different OLEDs and four different high power LEDs. The DC characteristics have shown that the OLEDs have a greater (more than double)

device, series and diode resistance than the LEDs. However, when using the voltage divider rule it has been shown that the modulating voltage across the emitting portion of the device is almost the same for all devices tested, between 8-13% with the exception of the Luxeon rebel at 23% when modulating from a voltage source. The bias current dependency on the modulation bandwidth for both LEDs and OLEDs has also been investigated. We have empirically demonstrated that an increase in bias current directly leads to an increase in the available modulation bandwidth of both types of device. However, distinct differences in the behaviour of each device have been outlined. For the LEDs, the bandwidth increases exponentially with bias current, tending towards a saturation limit. It has been shown for the four LED devices tested that ≥80% of the maximal available bandwidth is achieved within 35% of the maximum rated bias current, with the red LED showing the greatest results at just 17%. The OLEDs tested display a linear relationship between the bandwidth and the applied bias current. For this case, ≥80% of the maximal available bandwidth was achieved at ≥60% of their maximum rating.

ACKNOWLEDGMENT

This project is supported by UK EPSRC grant EP/P006280/1: MARVEL and the H2020 MSC ITN 764461 (VISION).

REFERENCES

[1] Z. Ghassemlooy, W. Popoola, and S. Rajbhandari, *Optical wireless communications: system and channel modelling with Matlab®*: CRC press, 2019.

[2] S. Rajbhandari, P. A. Haigh, Z. Ghassemlooy, and W. Popoola, "Wavelet-neural network VLC receiver in the presence of artificial light interference," *IEEE photonics technology letters,* vol. 25, pp. 1424-1427, 2013.

[3] J. Yang, Z. Liu, B. Xue, Z. Liao, J. Wang, and J. Li, "Visible light communication and lighting using laser diodes," in *2016 International Conference on Numerical Simulation of Optoelectronic Devices (NUSOD)*, pp. 83-84, 2016.

[4] P. d. Souza, N. Bamiedakis, K. Yoshida, P. P. Manousiadis, G. A. Turnbull, I. D. W. Samuel*, et al.*, "High-Bandwidth Organic Light Emitting Diodes for Ultra-Low Cost Visible Light Communication Links," in *2018 20th International Conference on Transparent Optical Networks (ICTON)*, pp. 1-4, 2018.

[5] W. N, Q. Y, W. W, T. S, and S. J, "Visible Light Communication based Intelligent Traffic Light System: Designing and Implementation," in *2018 Asia Communications and Photonics Conference (ACP)*, pp. 1-3, 2018.

[6] B. Gulbahar and S. Sencan, "Wireless Internet service providing for 5G with hybrid TV broadcast and visible light communications," in *2017 Wireless Days*, pp. 66-69, 2017.

[7] K. Kadam and M. R. Dhage, "Visible Light Communication for IoT," in *2016 2nd International Conference on Applied and Theoretical Computing and Communication Technology (iCATccT)*, pp. 275-278, 2016.

[8] H. Chun, S. Rajbhandari, G. Faulkner, D. Tsonev, E. Xie, J. J. D. McKendry*, et al.*, "LED Based Wavelength Division Multiplexed 10 Gb/s Visible Light Communications," *Journal of Lightwave Technology,* vol. 34, pp. 3047-3052, 2016.

[9] K. Werfli, P. Chvojka, Z. Ghassemlooy, N. B. Hassan, S. Zvanovec, A. Burton*, et al.*, "Experimental Demonstration of High-Speed 4 × 4 Imaging Multi-CAP MIMO Visible Light Communications," *Journal of Lightwave Technology,* vol. 36, pp. 1944-1951, 2018.

[10] I. Lu, C. Lai, C. Yeh, and J. Chen, "6.36 Gbit/s RGB LED-based WDM MIMO visible light communication system employing OFDM modulation," in *2017 Optical Fiber Communications Conference and Exhibition (OFC)*, pp. 1-3, 2017.

[11] P. A. Haigh, P. Chvojka, Z. Ghassemlooy, S. Zvanovec, and I. Darwazeh, "Non-Orthogonal Multi-band CAP for Highly Spectrally Efficient VLC Systems," in *2018 11th International Symposium on Communication Systems, Networks & Digital Signal Processing (CSNDSP)*, pp. 1-6, 2018.

[12] Z. Yingjun, L. Shangyu, C. Siyuan, X. Huang, and N. Chi, "2.08Gbit/s visible light communication utilizing power exponential pre-equalization," in *2016 25th Wireless and Optical Communication Conference (WOCC)*, pp. 1-3, 2016.

[13] R. Bian, I. Tavakkolnia, and H. Haas, "15.73 Gb/s Visible Light Communication With Off-the-Shelf LEDs," *Journal of Lightwave Technology,* vol. 37, pp. 2418-2424, 2019.

[14] Y. Zhou, J. Zhao, M. Zhang, J. Shi, and N. Chi, "2.32 Gbit/s phosphorescent white LED visible light communication aided by two-staged linear software equalizer," in *2016 10th International Symposium on Communication Systems, Networks and Digital Signal Processing (CSNDSP)*, pp. 1-4, 2016.

[15] Z. N. Chaleshtori, P. Chvojka, S. Zvanovec, Z. Ghassemlooy, and P. A. Haigh, "A Survey on Recent Advances in Organic Visible Light Communications," in *2018 11th International Symposium on Communication Systems, Networks & Digital Signal Processing (CSNDSP)*, pp. 1-6, 2018.

[16] P. A. Haigh, Z. Ghassemlooy, I. Papakonstantinou, and H. Le Minh, "2.7 Mb/s with a 93-kHz white

organic light emitting diode and real time ANN equalizer," *IEEE Photonics Technology Letters,* vol. 25, pp. 1687-1690, 2013.

[17] P. A. Haigh, Z. Ghassemlooy, I. Papakonstantinou, F. Arca, S. F. Tedde, O. Hayden*, et al.*, "A 1-Mb/s visible light communications link with low bandwidth organic components," *IEEE photonics technology letters,* vol. 26, pp. 1295-1298, 2014.

[18] S. T. Le, T. Kanesan, F. Bausi, P. Haigh, S. Rajbhandari, Z. Ghassemlooy*, et al.*, "10 Mb/s visible light transmission system using a polymer light-emitting diode with orthogonal frequency division multiplexing," *Optics letters,* vol. 39, pp. 3876-3879, 2014.

[19] P. A. Haigh, F. Bausi, T. Kanesan, S. T. Le, S. Rajbhandari, Z. Ghassemlooy*, et al.*, "A 20-Mb/s VLC link with a polymer LED and a multilayer perceptron equalizer," *IEEE Photonics Technology Letters,* vol. 26, pp. 1975-1978, 2014.

[20] P. A. Haigh, F. Bausi, H. Le Minh, I. Papakonstantinou, W. O. Popoola, A. Burton*, et al.*, "Wavelength-multiplexed polymer LEDs: Towards 55 Mb/s organic visible light communications," *IEEE Journal on Selected Areas in Communications,* vol. 33, pp. 1819-1828, 2015.

[21] H. Chen, Z. Xu, Q. Gao, and S. Li, "A 51.6 Mb/s experimental VLC system using a monochromic organic LED," *IEEE Photonics Journal,* vol. 10, pp. 1-12, 2017.

[22] P. Deng, M. Kavehrad, and M. A. Kashani, "Nonlinear modulation characteristics of white LEDs in visible light communications," in *2015 Optical Fiber Communications Conference and Exhibition (OFC)*, pp. 1-3, 2015.

[23] X. Li, Z. Ghassemlooy, S. Zvanovec, M. Zhang, and A. Burton, "Equivalent Circuit Model of High Power LEDs for VLC Systems," in *2019 2nd West Asian Colloquium on Optical Wireless Communications (WACOWC)*, pp. 90-95, 2019.

[24] P. Horowitz and W. Hill, *The art of electronics*: Cambridge Univ. Press, 1989.

[25] G.-J. A. Wetzelaer and P. W. Blom, "Diffusion-driven currents in organic-semiconductor diodes," *NPG Asia Materials,* vol. 6, p. e110, 2014.

[26] J. M. Shah, Y.-L. Li, T. Gessmann, and E. F. Schubert, "Experimental analysis and theoretical model for anomalously high ideality factors (n≫ 2.0) in AlGaN/GaN pn junction diodes," *Journal of Applied Physics,* vol. 94, pp. 2627-2630, 2003.

[27] A. Burton, Z. Ghassemlooy, S. Zvanovec, P. A. Haigh, H. L. Minh, and X. Li, "Investigation into Using Compensation for the Nonlinear Effects of the Output of LEDs in Visible Light Communication Systems," in *2019 2nd West Asian Colloquium on Optical Wireless Communications (WACOWC)*, pp. 80-84, 2019.

[28] H. Elgala, R. Mesleh, and H. Haas, "Impact of LED nonlinearities on optical wireless OFDM systems," in *21st Annual IEEE International Symposium on Personal, Indoor and Mobile Radio Communications*, pp. 634-638, 2010.